MIMO Attitude Control for a Spinning Rocket

W. C. Leite Filho[1], J. Guimaraes and L. Galembeck

Abstract This work studies the performance of a nonlinear Multiple-Input-Multiple-Output (MIMO) controller with roll input as a strategy applied to the control of a sounding rocket with no direct roll control and a parabolic residual spin. Its performance is compared to two regular linear Single-Input-Single-Output (SISO) controllers applied separately on the yaw and pitch command paths with respect to step response and the ability to follow a design trajectory, both under ideal circumstances and under simplified wind perturbations. Simulation results show that the MIMO controller presents similar step response to the SISO strategy, but its ability to take coupling into account leads to a better trajectory behavior. However, the MIMO controller is less robust to changes in the predicted residual spin and may introduce a stable but oscillating effect to the system's behavior.

Keywords. Spinning rocket. MIMO control design. Spacecraft attitude control.

1. Introduction

When dealing with rockets that present no direct roll control, it is possible that disturbances along the system may introduce some roll rate [10]. The highly coupled nature of the rocket's equations of motion make the study of its dynamic a very complex subject [7, 9]. It is necessary to understand how well a given control system is able to deal with such perturbations.

In this paper, we are interested in studying the performance of a multiple-input-multiple-output (MIMO) controller with roll input and how it compares to a single-

[1] Instituto Nacional de Pesquisas Espaciais - INPE

São José dos Campos, Brazil

Email: waldclf@gmail.com

input-single-output (SISO) PID controller when used on a rocket under the influence of an uncontrolled spin rate of parabolic profile. The controllers are compared by analyzing both step response and the ability to send the system to a pre-determined trajectory, with and without the influence of wind perturbations.

2. Mathematical Model

Given the presence of uncontrolled spin, it is necessary to consider the complete equations of motion for a sounding rocket with thrust vectoring. The equations are initially derived for the body reference frame, and later related to the inertial reference frame through Euler's differential equations.

The complete motion of the vehicle, as described in the body reference, is given by the set of equations (2.1).

$$\begin{cases} \dot{u} = -\left(\dfrac{C_d P_d S}{m}\right) + \dfrac{T}{m} - g\cos\theta\cos\psi - qw + r \\ \dot{v} = -Y_\beta \beta + Y_{\beta_y}\beta_y - g(\sin\theta\sin\phi - \cos\theta\sin\psi\cos\phi) - ru + pw \\ \dot{w} = -Z_\alpha \alpha - Z_{\beta_z}\beta_z - g(\sin\theta\cos\phi - \cos\theta\sin\psi\sin\phi) - pv + qu \\ \dot{p} = -L_p p + \dfrac{I_{yy} - I_{zz}}{I_{xx}} qr \\ \dot{q} = -M_q q + \dfrac{I_{zz} - I_{xx}}{I_{yy}} pr + M_\alpha \alpha + M_{\beta_z}\beta_z \\ \dot{r} = -N_r r + \dfrac{I_{xx} - I_{yy}}{I_{zz}} pq - N_\beta \beta + N_{\beta_y}\beta_y \end{cases} \tag{2.1}$$

The relationship between the angular velocities in the body reference frame and the Euler angles (for a rotation sequence of θ-ψ-ϕ) is given by the set of equations (2.2).

$$\begin{cases} \dot{\phi} = p - q\tan\psi\cos\phi + r\tan\psi\sin\phi \\ \dot{\theta} = q\dfrac{\cos\phi}{\cos\psi} - r\dfrac{\sin\phi}{\cos\psi} \\ \dot{\psi} = q\sin\phi + r\cos\phi \end{cases} \tag{2.2}$$

If the rocket has no spin rate (p=0), the equations can be decoupled and the system becomes completely independent in the θ and ψ directions.

2.1 Resolver

When it comes to real implementation on a spinning rocket, one must consider how the sensors measurements for a given direction correspond to the real Euler angles that describe the vehicle's attitude. In order to relate the measured errors to the modeled angles, a resolver must be used. Its implementation is illustrated by Fig. 2.1.

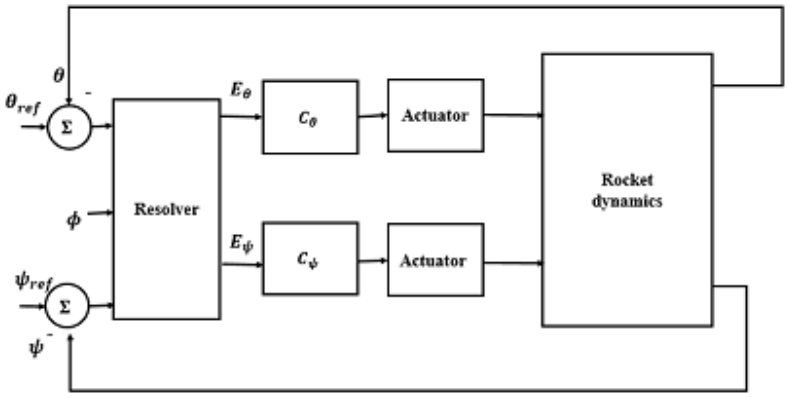

Fig. 2.1. Resolver implementation

For small values of ψ, its behavior can be represented by the set of equations (1.3).

$$\begin{cases} E_\theta = (\theta_{ref} - \theta)\cos\phi + (\psi_{ref} - \psi)\sin\phi \\ E_\psi = (\theta - \theta_{ref})\sin\phi + (\psi_{ref} - \psi)\cos\phi \end{cases} \tag{1.3}$$

3. Control Strategies

This paper considers two different control strategies to deal with the residual spin: the first is a decoupled system for pitch and yaw, with two independent single-input-single-output (SISO) controllers and the second, a coupled multiple-input-multiple-output (MIMO) controller.

3.1 Single-Input-Single-Output (SISO)

The initial control strategy consists of two independent PID controllers, designed separately and without taking the spin and other possible interactions into account. Given the symmetry of the vehicle, the same gains are used for pitch and yaw.

The main advantage in the use of SISO controllers rests on its simplicity and well known techniques of gain design [6]. However, it is possible this system is unable to control the real spinning rocket, depending on the rate of rotation.

Fig. 3.1 illustrates a PID SISO controller applied in conjunction with an actuator.

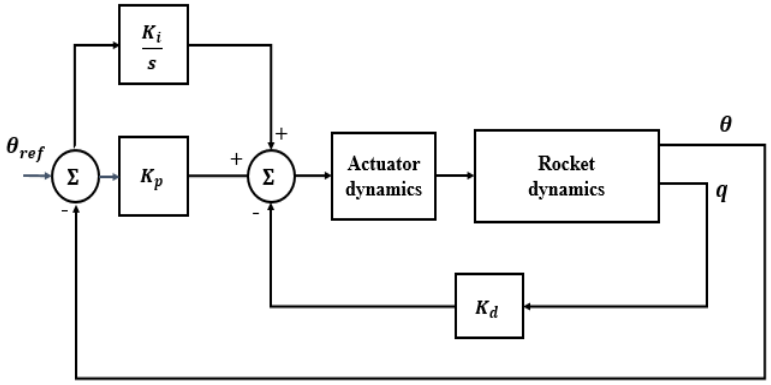

Fig. 3.1. SISO classic PID control scheme

3.2 Multiple-Input-Multiple-Output (MIMO)

Multiple-Input-Multiple-Output controllers allow for better control over interdependent variables [8] and are useful in problems where coupling is relevant.

In its most general formulation when applied to a rocket, a MIMO controller would consider the reference signals to both pitch and yaw simultaneously and generate a control law that attempts to negate the cross-terms, as seen in [10]. However, this approach does not consider the roll rate directly.

The control system proposed here considers a nonlinear MIMO controller that uses not only pitch and yaw measurements but also the roll measurement. It consists of a PID structure for the direct branch and a PD structure for the cross branch. The cross portion of the control signal is then multiplied by the spin rate measured, as well as a fixed gain G. Fig. 3.2 illustrates the structure used for the pitch control signal.

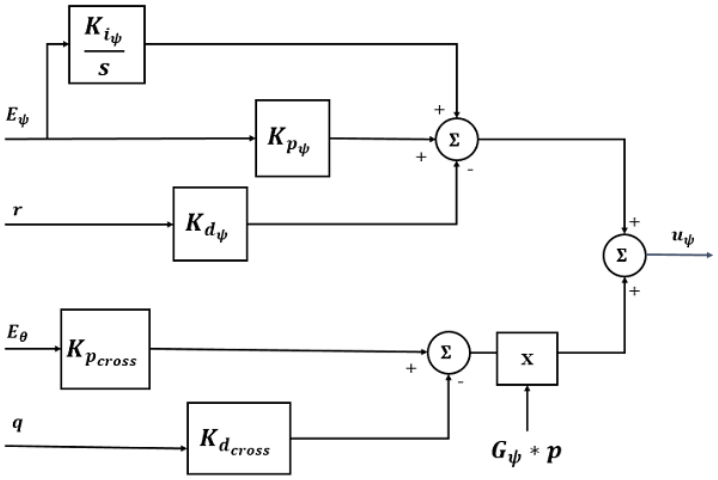

Fig. 3.2. MIMO structure for yaw control.

4. Case Study

The vehicle studied presents a design residual spin rate that follows a parabolic profile given by equation (4.1).

$$p(t) = \frac{t^2}{30}[\text{deg}/\,s] \tag{4.1}$$

As part of the design requirements, the step response for the controller should present a settling time of less than four seconds, an overshoot of less than 40% and the smallest ramp error possible. Given structural and physical limitations, it is also required that the control command never surpasses 4 degrees and that the rising time is larger than 0.5 second.

For simulation purposes, the actuator used will be modeled by a first order system with ω =4,5Hz.

4.1 SISO Controller Gains

Since the vehicle's parameters change constantly throughout the flight, there must be an appropriate gain scheduling. The PID gains for the SISO approach were tuned

in 1-second intervals using the step and ramp requirements. It is important to understand that those requirements are often contradictory, so eventual trade-offs were made.

The tuning strategy used starts with the critical flight condition, that is, the instant where M_α is maximum, and the gains are calculated so that setting time and minimum ramp error are prioritized. Then, the gains are scheduled using the ratio of thrust coefficients with respect to the critical time, as well as performance metrics.

The gains calculated for the SISO controller are shown in Fig. 4.1. The integral part of the controller is not used for the first five seconds, in order to avoid eventual liftoff errors.

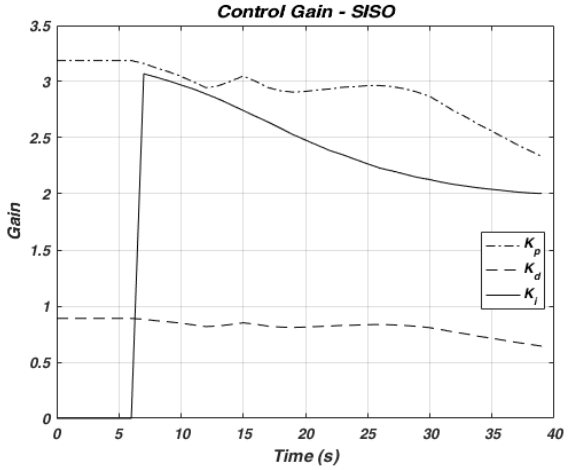

Fig. 4.1. Control Gains – SISO Controller

4.2 MIMO Controller Gains

For the purpose of comparison, the direct gains for the MIMO controller were considered the same as the SISO case, shown in Figure 4. The cross gains for the MIMO controllers were calculated using the nonconvex nonsmooth optimization algorithms described in [2], [3], [4] and [5] through the MATLAB function *systune*.

The gains were tuned so that the system showed the desired step response. The tuning requirements used that resulted in the best results were gain margin of 5dB, phase margin of 30º, a 20% maximum overshoot and a natural frequency close to the SISO step response. During the tuning for each time snapshot, the roll gain was considered unitary (i.e. G_θ=-1 and G_ψ=+1). Figure 4.2 shows the cross gains calculated through this method.

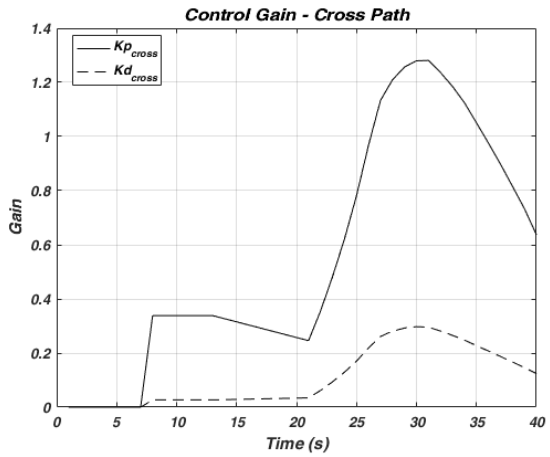

Fig. 4.2. Control Gains – MIMO – Cross Path.

5. Performance Analysis

For comparing the two control systems, their performance was first analyzed with respect to their separate pitch and yaw step response for the critical time, both in ideal conditions and under wind perturbation. Then, the ability to follow the design trajectory with respect to its Euler angles was studied under both conditions. In both cases, the wind perturbation was modelled by a simplified model as a half-sine of 10m/s of amplitude and a 2 second half-period.

5.1 Step Response

The step response for the critical time when M_α is maximum (t=30s) can be seen on Fig. 5.1 and Fig. 5.2. Fig. 5.3 and Fig 5.4 show the corresponding step response for a negative roll rate that follows the same parabolic profile. For the purpose of the step response analysis, the roll gain G was considered unitary and steps were applied separately to each angle reference.

The step response for the MIMO controller, in part due to the tuning process used, is quite similar to the SISO controller. The angle not receiving the step reference shows small oscillations under the MIMO controller, due to the initial large error of the step angle stimulating the cross path.

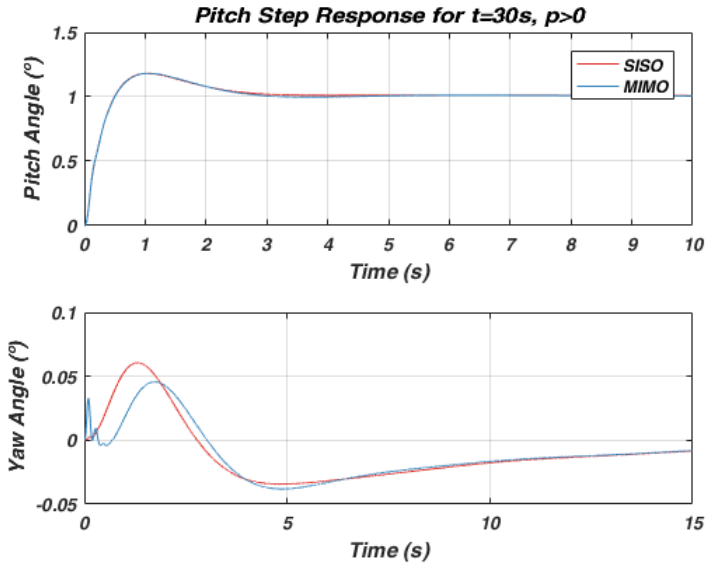

Fig. 5.1. Pitch Step Response for Critical Time (t=30s) – p>0.

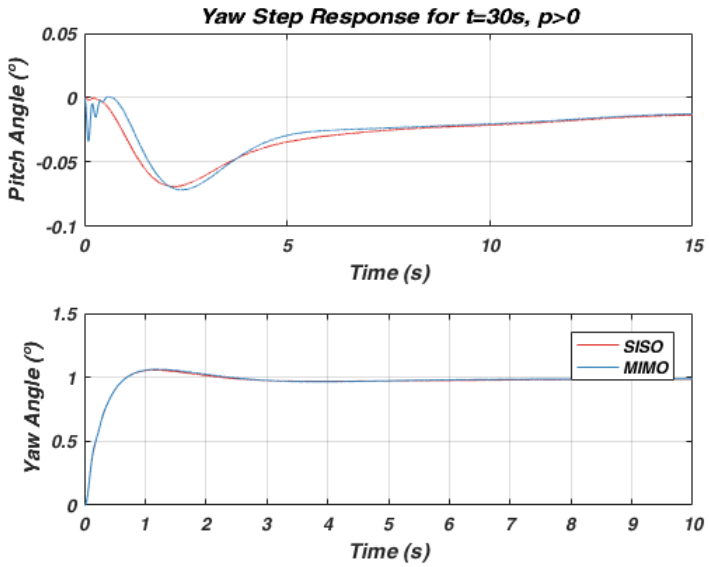

Fig. 5.2. Yaw Step Response for Critical Time (t=30s) – p>0.

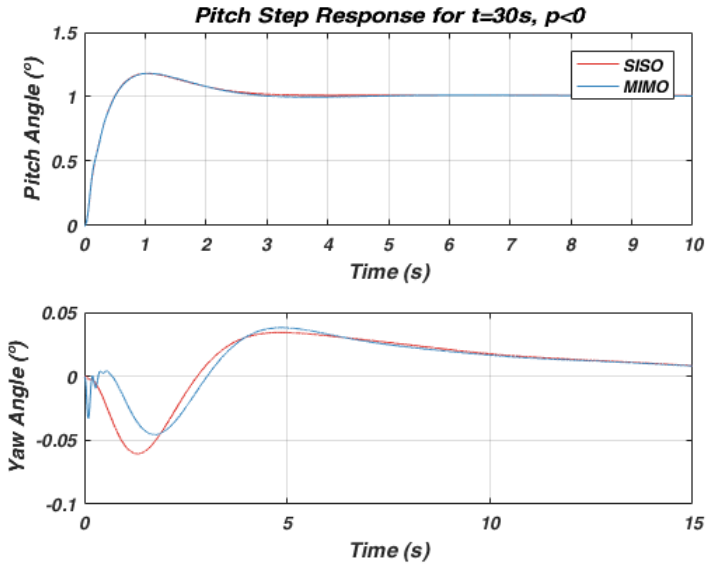

Fig. 5.3. Pitch Step Response for Critical Time (t=30s) – p<0.

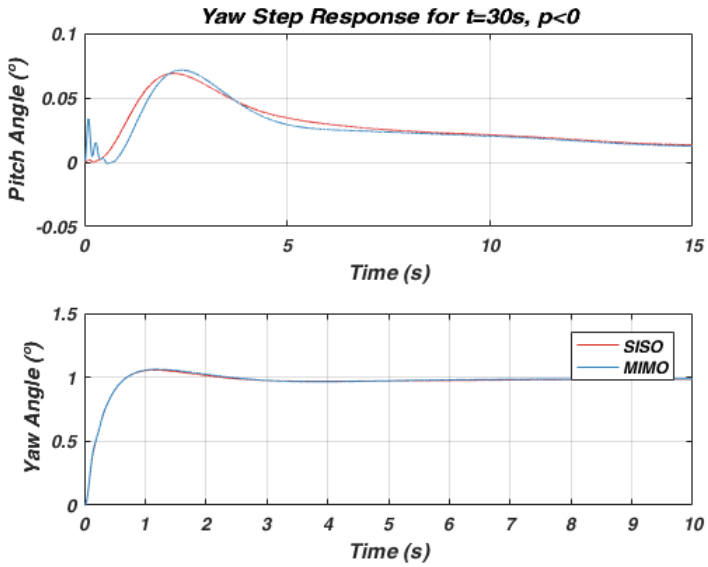

Fig. 5.4. Yaw Step Response for Critical Time (t=30s) – p<0.

The step requirements presented on section 4 are respected for each time snap-shot even with the MIMO controller, with raising time larger than 0.5s, overshoot

smaller than 40% and settling time smaller than 4s for each variable under the step reference. Finally, the step response of the stimulated angle showed no undershoot for any time considered, which is desired for this kind of thrust vectoring control (TVC).

5.2 Step Response Under Wind Perturbation

The wind perturbation analysis to the step response considers a gust wind applied at the start of the simulation.

The influence of the wind on the pitch step response can be seen on Fig. 5.5 and Fig. 5.6.

The effect on the yaw step response is similar. Both images show how the rocket would respond to such perturbations if there were no roll, in which case the two controllers would be equivalent.

It is possible to see that the MIMO controller responds well to the wind perturbations applied. Once again, small oscillations can be seen at the start, but after that the MIMO step response on the opposite angle seems to be either equal or slightly better than the SISO one. The SISO controller creates a higher overshoot on the opposite angle during the transient response.

It is important to note that in both cases the magnitude of the perturbation on the opposite channel is relatively small.

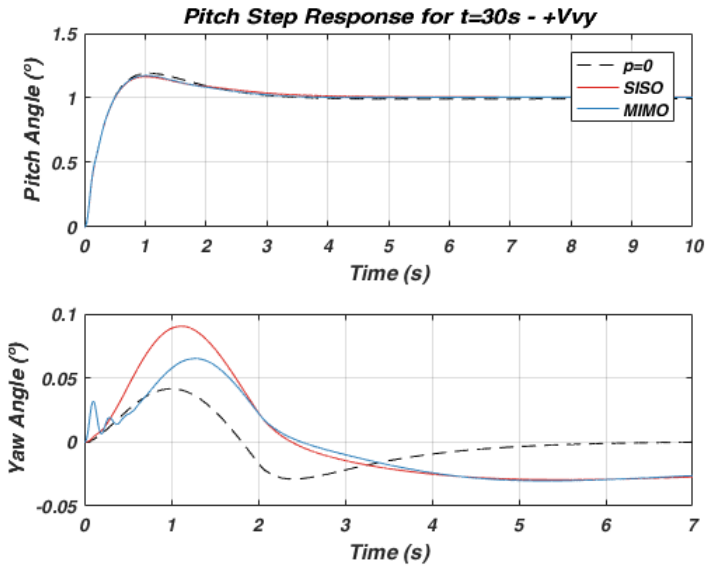

Fig. 5.5. Pitch Step Response for Critical Time (t=30s) under Wind Perturbation - Vvy.

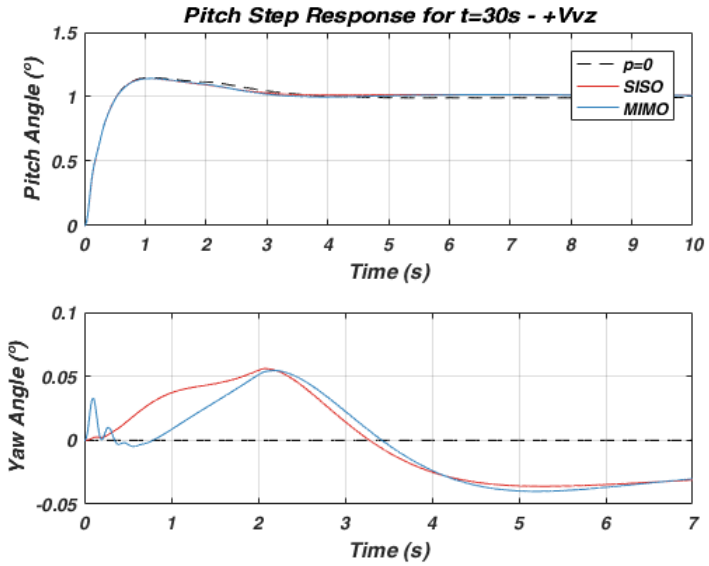

Fig. 5.6. Pitch Step Response for Critical Time (t=30s) under Wind Perturbation - Vvz.

5.3 Design Trajectory

Initially, the MIMO roll gains were considered, once again, unitary. Fig. 5.7 shows how well the controllers lead the vehicle to a design trajectory for a positive spin rate, while Fig. 5.8 refers to a negative spin rate.

Both controllers have a very similar response to the pitch reference signal, being almost interchangeable. The main difference appears on the yaw response.

While the reference signal for the yaw angle is zero, the SISO controller shows a drift under residual spin. This drift is mainly due to the integrator term, but that cannot be removed without affecting the step requirements unfavorably.

The MIMO controller is able to improve on this factor. In fact, for unitary roll gains, as a measure of the error on the yaw channel it is possible to see a reduction of 12.77% in the area under the yaw curve for the MIMO controller.

5.3.1 Influence of Roll Gain

An increase in the roll gains actually reduces the area under the curve. For instance, with G_θ=-2.5 and G_ψ=+2.5, the reduction in area becomes 27.66% when compared to the SISO case.

Further analysis shows that, for these direct and cross path gains, the maximum value of roll gains for which the system is stable is 3.

This actually means the controller behaves well for this parabolic spin rate profile when the product between p and G is smaller than this value. Smaller values of G provide bigger leeway if there is uncertainty about the maximum roll, but the drift on the yaw angle will be larger.

Fig 5.9 shows the design trajectory for G_θ=-3.2 and G_ψ=+3.2, when the system response is clearly unstable.

This indicates that, while the SISO controller has worse performance as far as the yaw drift, it is stable for larger values of spin. If there is relative certainty about the maximum residual roll encountered and its profile, the MIMO strategy provides better results. However, if it is possible for the vehicle to encounter a very different residual roll when compared to the design roll profile, the SISO controller is more robust and, therefore, preferable.

Finally, even when stable, the MIMO system shows a more prominent oscillatory behavior than the one encountered with the SISO strategy. It is possible, though, that this occurs in consequence of the method used for gain calculation.

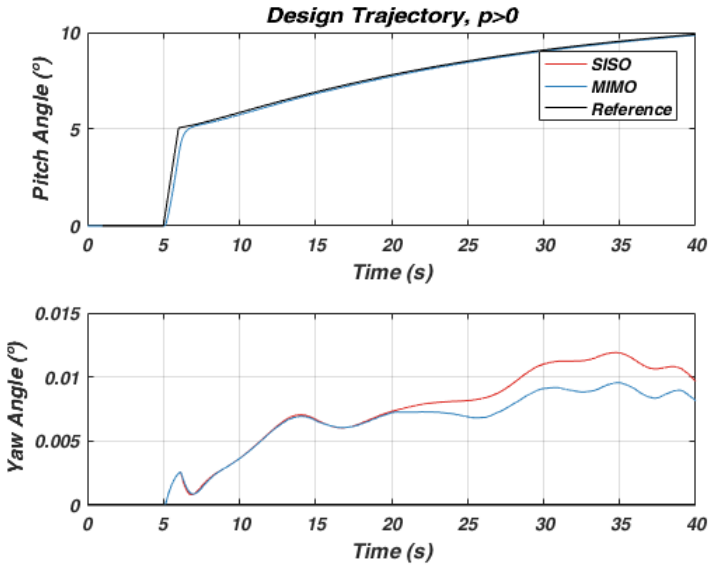

Fig. 5.7. Design Trajectory - G_θ=-1 and G_ψ=+1 – p>0.

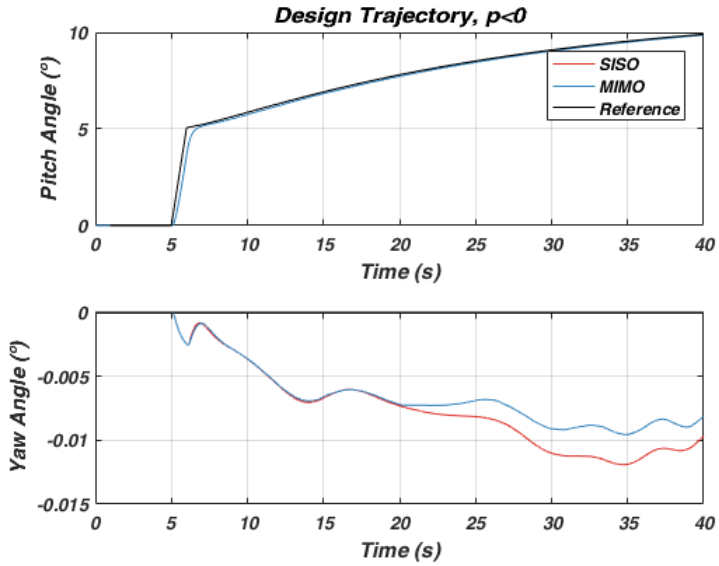

Fig. 5.8. Design Trajectory - G_θ=-1 and G_ψ=+1 – p<0.

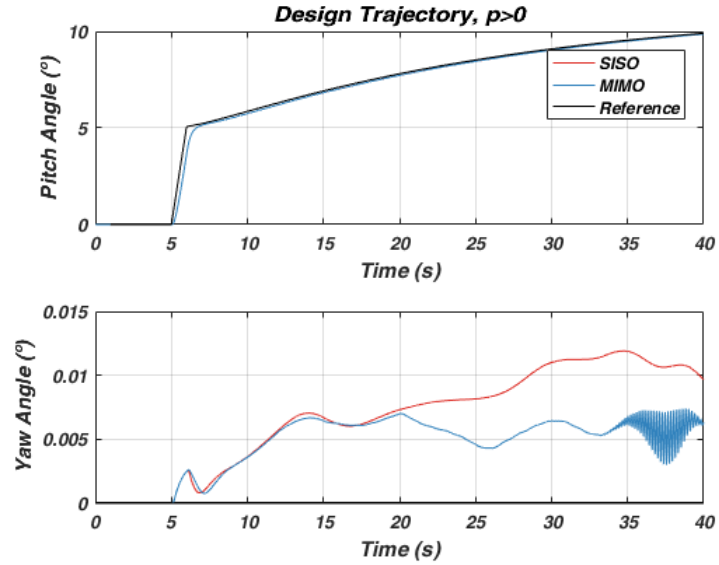

Fig. 5.9. Design Trajectory - G_θ=-3.2 and G_ψ=+3.2.

5.4 Design Trajectory Under Wind Perturbation

The influence of wind perturbation on the design trajectory was also analyzed. In this case, the wind profile used was based on [1] and varies with the vehicle's altitude.

Fig. 5.10 shows the simulated behavior for a controller with unitary roll gain in the MIMO case, as compared to the previous analyzed SISO controller. Both controllers are stable, but the MIMO strategy presents a smaller drift on the yaw channel when compared to the SISO controller, in the same manner as the results of section 5.3.

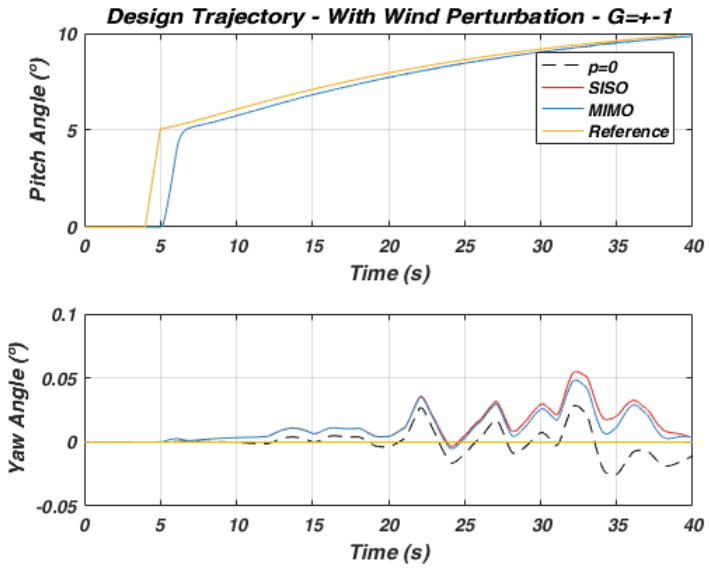

Fig. 5.10. Design Trajectory under Wind Perturbation - G_θ=-1 and G_ψ=+1.

6. Conclusion

This paper studies how well a nonlinear MIMO controller with roll input is able to improve the performance of a linear SISO controller when applied to a spinning rocket with no roll control.

The performance metrics used indicate the MIMO strategy shows improvement with respect to ability to follow the design trajectory while presenting similar step response. The controller's behavior was also favorable when under perturbation of a gust wind.

The MIMO controller, however, is more susceptible to eventual variations in the predicted residual spin, with its apparent robustness being related to the roll gain used on the cross path.

Finally, in this paper, the gains calculated for the MIMO controller were not designed taking robust control theory into account and, therefore, one can only guarantee its behavior with respect to the tuned flight conditions, and not its overall robustness.

Further studies should consider how a variable roll gain changes the MIMO controller performance, and different methods of gain calculation should be tested in an attempt to improve the step response in such a way that robustness is also ensured.

References

1. Adelfang, S. I. Simulation of Wind-Profile Perturbations for Launch-Vehicle Design. J Spacecr Rockets. doi: 10.2514/1.3271
2. Apkarian P, Noll D (2006). Nonsmooth H-infinity Synthesis. IEEE Trans Autom Control 51:71-86
3. Apkarian P, Noll D (2007). Nonsmooth Optimization for Multiband Frequency-Domain Control Design. Automatica 43:724–731.
4. Apkarian P, Gahinet P, Buhr C (2014). Multi-model, multi-objective tuning of fixed-structure controllers. Proc Eur Control Conf. doi: 10.1109/ECC.2014.6862200
5. Apkarian, P, Dao MN, Noll D (2015). Parametric Robust Structured Control Design. IEEE Trans Autom Control. doi: 10.1109/TAC.2015.2396644
6. Garner D (1964). Control Theory Handbook. NASA Marshall Space Flight Center, NASA TM X-53036.
7. Mohammadloo S, Alizadeh MH, Jafari M (2014). Multivariable Autopilot Design for Sounding Rockets Using Intelligent Eigenstructure Assignment Technique. Proc Int J Control Autom Syst. doi: 10.1007/s12555-012-0229-4
8. Pothukuchi RP et al (2016). Using Multiple Input, Multiple Output Formal Control to Maximize Resource Efficiency in Architectures. Proc Int Symp Comp Architecture. doi: 10.1109/ISCA.2016.63
9. Sun BC, Ryu JH, Tahk MJ (1996). Robust Control Design for Spinning Rocket. Proc Soc Instrum Control Eng Annu Conf. doi: 10.1109/SICE.1996.865460
10. White J (1991). Attitude Control of a Spinning Rocket via Thrust Vectoring. Proc Navig Control Conf. doi: 10.2514/6.1991-2617